



COB-2021-1228

THERMAL PERFORMANCE ANALYSIS OF AN ULTRA-THIN LOOP HEAT PIPE FOR ELECTRONIC COOLING APPLICATION

Kelvin Guessi Domiciano

Larissa Krambeck

Juan Pablo Florez Mera

Marcia Barbosa Henriques Mantelli

Department of Mechanical Engineering, Federal University of Santa Catarina, Florianópolis/SC, 88040-900, Brazil
kelvin.guessi@labtucal.ufsc.br; larissa.krambeck@labtucal.ufsc.br; jpablo@labtucal.ufsc.br; marcia@labtucal.ufsc.br

Abstract. A flat ultra-thin loop heat pipe (UTLHP) is experimentally developed and investigated in the present study. Sintering and diffusion bonding technology are used to manufacture the device with a thin thickness. The ultra-thin loop heat pipe consists of 76 mm x 60 mm composed of three flat copper sheets, totalizing the thickness of 1.6 mm. The device presents a primary wick structure located at the evaporator and a secondary wick structure located at the liquid line to promote the working fluid return to the heated side. Both porous media consists of sintered copper powder. Water is used as the working fluid. A workbench is developed to simulate the operating condition and the geometric characteristics of a chip mobile electronic processor with 1 cm², a typical application, to evaluate the ultra-thin loop heat pipe thermal performance at the horizontal position. The condenser is cooled by natural air convection. The experimental analysis showed that the UTLHP operates effectively, starting to work at low heat flux (3 W/cm²) with an evaporator temperature of 56.2 °C. The device revealed a minimum thermal resistance of 1.05 °C/W at 8 W/cm². The experimental results proved that the device is suitable for electronic cooling applications of miniature devices, working with an evaporator temperature below 100 °C.

Keywords: ultra-thin loop heat pipe, diffusion bonding of UTLHPs, electronic application.

1. INTRODUCTION

Heat transfer devices that involve the phase change of a working fluid have excellent heat transport characteristics. They can transfer a large amount of heat passively between a source and a sink. The heat source, sometimes of small dimensions, can be, for instance, electronic chips from a CPU processor of mobile phones, tablets, smartwatches, or notebooks. Heat can be removed from the condenser by several mechanisms, including natural air convection, forced air convection (fans) or water cooling (pumps).

Heat pipes (HPs) can operate in a wide range of temperatures, enabling different heat transfer applications. Appropriate material and working fluid must be selected according to the temperature level. For electronics applications, high heat flux levels (such as 104 W/cm²) can be observed in the evaporator, usually delivered in larger condenser surface areas. In this case, the devices operate as heat spreaders, where a larger area can ultimately remove the heat by natural convection and single-phase cooling systems (BEJAN; KRAUS, 2003). Specifically, in mobile electronic applications, the average size and heat flux can reach 100 mm² and 13.65 W/cm², as shown in Table 1.

Table 1. Present chip processors specifications (WIKICHIP, 2021).

Chip processor	Chipset size [mm ²]	Thermal design power [W]	Heat flux [W/cm ²]
Snapdragon 855	73.27	10	13.65
Kirin 990 5G+	113.31	6	5.26
A12X Bionic	122.00	6	4.92
A14 Bionic	88.00	6	6.82
Exynos 9820	127.00	9	7.09

Several researchers studied potential cooling solutions for electronics systems, including heat pipes coupled with heat spreader plates, fans, or heat sinks (NGUYEN *et al.*, 2000; VASILIEV, 2008). The heat pipe technology exhibits a heat transfer performance superior to high conductivity materials (spreader), ensuring an effective solution for cooling electronics devices. Vasiliev *et al.* (2008) developed two miniature copper heat pipes with a total thickness of 5 mm and

6 mm for a CPU cooling system. The HPs successfully dissipated 80 W for 6 mm and 60 W for 5 mm, keeping the adiabatic temperature below 90 °C with a total thermal resistance of 0.2 °C/W.

Despite all advantages of heat pipes, the wick might not provide the necessary liquid pumping for the device orientated against gravity (evaporator located above the condenser). In these cases, the heat transfer efficiency abruptly decreases. To compensate this problem, additional capillary pressure could be provided by reducing the effective pore radius of the wick. However, this solution may increase the hydraulic resistance, which is proportional to the square of the pore radius (MAYDANIK, 2005).

To overcome some disadvantages of conventional heat pipes, its sections were disjointed and the evaporator and condenser are separated through transport lines, resulting in Loop Heat Pipes (LHPs). The main characteristic of a LHP is the separation of the working fluid phases, vapor and liquid. The capillary structure is usually located inside the evaporator. However, for small devices, the wick structure can also be extended into the liquid line, called the liquid line wick. One great advantage of these devices is that the geometry of the evaporator can be designed separately from that of the condenser, which makes them more adjustable to the application.

Aiming mobile phone applications, LHPs need to be thin and compact. Zhou *et al.* (2017) investigated the efficiency of a loop heat pipe with an 0.8 mm thick evaporator manufactured by compressing a 2 mm cylinder. They used a wick structure made of sintered copper and water as the working fluid. The results showed that the optimal filling ratio is obtained when the wick structure is saturated with liquid. This charging ratio provided a temperature difference between the evaporator and condenser of 3.7 °C and thermal resistance of 0.29 K/W. Tang *et al.* (2018) studied the advances and applications of miniaturized loop heat pipes with flat evaporators. The authors concluded that the limitations of this technology were related to the low pumping capacity of the capillary structures and the difficulties related to their fabrication, especially the welding processes, resulting in high cost and low efficient devices.

As the LHP thickness becomes thinner, its heat transfer performance decreases because of the higher percentage of parasitic heat transfer rate from the evaporator to the liquid line or compensation chamber and higher confinement for the fluid flow. Despite many efforts to accomplished the fabrication of miniaturized LHPs, only a few studies showed successful results. To meet the requirement for mobile electronics application, the main objective of this study is to design, fabricate and evaluate the thermal performance of an ultra-thin loop heat pipe (UTLHP), working in horizontal orientation (negligible gravity effect) under natural air convection.

2. UTLHP FABRICATION

As remarked, the target application of the studied UTLHP is to remove heat from chip processors of mobile electronics. Therefore, the external dimensions of the constructed UTLHP are 76 x 60 mm and 1.6 mm in thickness. The proposed ultra-thin LHP is fabricated by diffusion bonding using three copper plates.

Figure 1(a) shows a schematic of the UTLHP's copper plates, with two surface plates of 0.3 mm in thickness and an inner layer with a thickness of 1 mm. This procedure results in low deformation devices that avoid the reduction of their thermal performance and lifespan (TANG *et al.*, 2018).

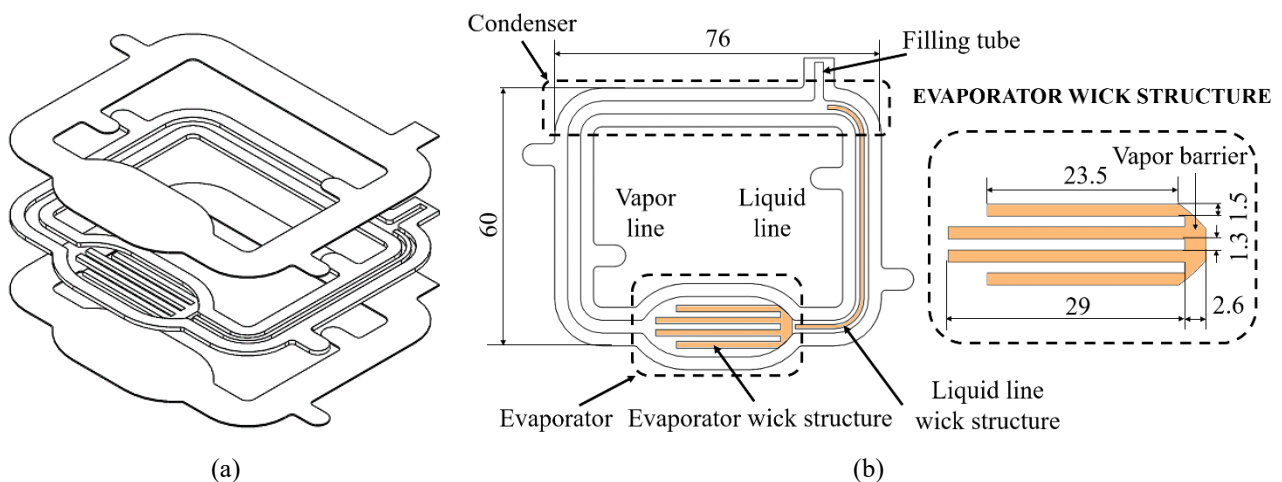


Figure 1. Schematic of the proposed: (a) UTLHP's copper plates (b) UTLHP's specifications. Dimension in mm.

The UTLHP is primarily composed of seven components: evaporator, evaporator wick structure, vapor line, condenser, liquid line, liquid line wick structure and a charging tube for filling the working fluid, as shown in Figure 1(b). There is not compensation chamber in this prototype, to avoid heat leaks and to save space.

Two sintered copper powder wicks, located at the evaporator and the liquid line wick structures, maintain the appropriate operation of the UTLHP. Before the diffusion bonding, both porous media with a thickness of 1 mm, were

sintered. The first wick, located at the evaporator, promotes the capillary force that is responsible for suppressing the total pressure drop. It is constituted by four branches in teeth format, with 1.5 mm of width. This shape directs the vapor to the vapor line, using vapor grooves of 1.3 mm width. Besides that, a vapor barrier of approximately 2.6 mm in length prevents the vapor to flow back to the liquid line. The liquid line wick structure keeps wet the heated side by supplying the liquid from the condenser to the evaporator, which has the same geometry as the liquid line with 1 mm width, located in the center. The characteristics of the porous media are shown in Table 2.

Table 2. Properties of the copper sintered porous media (MERA, 2016).

Properties	Powder C
Particle average diameter [μm]	49.72
Porosity [%]	53.46 ± 3.87
Effective thermal conductivity [W/m.K]	252.00
Permeability [m^2]	$1.99 \times 10^{-12} \pm 1.02$
Effective porous radio [μm]	21.04 ± 2.2

After the diffusion bonding process, the UTLHP was cleaned with acetone and evacuated. Figure 2 shows the prototype of the UTLHP after the cleaning procedure. In the sequence, the heat exchanger was filled with the working fluid. Preliminary tests showed that the filling ratio (FR) of 30% provides the best thermal results when degassed distilled water is used as the working fluid. The FR is defined as the ratio between the volume of the working fluid and the total internal void volume of the UTLHP. Table 3 lists the main specifications of the proposed ultra-thin flat loop heat pipe.

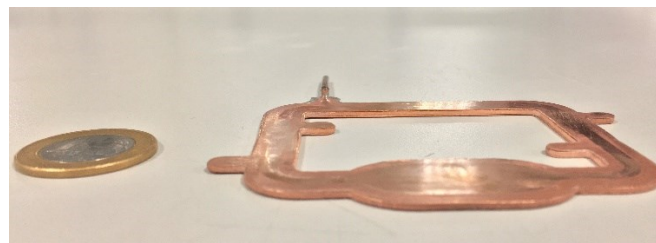


Figure 2. The prototype of the UTLHP.

Table 3. The main specifications of the ultra-thin loop heat pipe.

UTLHP	Parameter	Dimension
Evaporator	Size (LxW)	37.5 mm x 20 mm
	Heating area (LxW)	10 mm x 10 mm
Evaporator wick	Size (LxW)	23.5 mm x 1.5 mm / 29 mm x 1.5 mm
Vapor grooves	Size (LxW)	23.5 x 1.3 mm
Liquid line wick	Size (LxW)	70.49 mm x 1 mm
Vapor line	Channel size (LxW)	79.17 mm x 3 mm
Liquid line	Channel size (LxW)	79.17 mm x 3 mm
Condenser	Channel size (LxW)	46 mm x 3 mm
Working fluid	Distilled water	0.32 ml (FR 30%)

3. EXPERIMENTAL SETUP

Figure 3(a) presents the experimental setup used for the thermal tests. The experimental apparatus consists of a power supply unit, a data acquisition system (*DAQ-NITM SCXI-1000*), temperature sensors (*Omega EngineeringTM*) and a computer. T-type thermocouples evaluate the temperatures on the external surface of the UTLHP, fixed by thermosensitive adhesive strip *KaptonTM*, as the positions shown in Figure 3(b). There are thermocouples at the heating zone of the evaporator (T_1), the evaporator exit (T_2), the condenser region (T_3 , T_4 and T_5) and the evaporator entry (T_6). Moreover, there is a thermocouple that monitors the ambient temperature (T_{amb}).

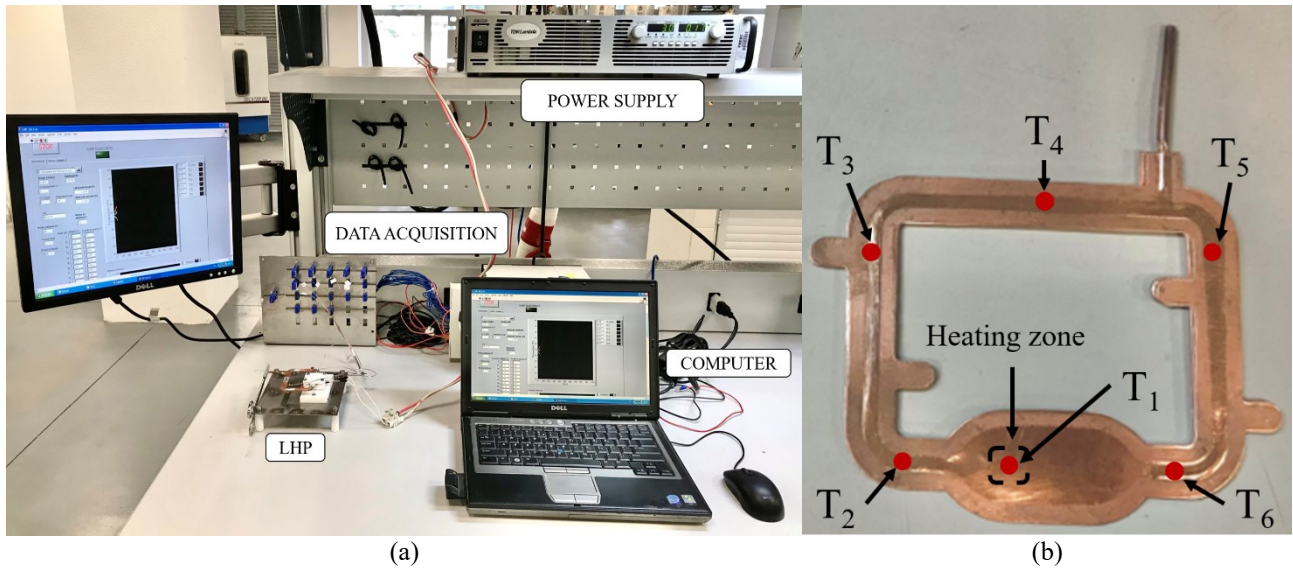


Figure 3. Experimental testing system: (a) Experimental apparatus (b) Thermocouple distribution.

A workbench is developed to simulate the operating condition and the geometric characteristics of a chip electronic processor, with 1 cm², according to Table 1. Thus, the evaporator is heated by the Joule effect of an electrical resistor inside a copper block - Figure 4(a). The cartridge electrical resistor can dissipate 32 W and has a diameter of 3.2 mm and a length of 25 mm. Polytetrafluoroethylene (PTFE polymer) isolates the evaporator section from the external ambient. The condenser is cooled by natural air convection. The workbench with the UTLHP is detailed in Figure 4(b).

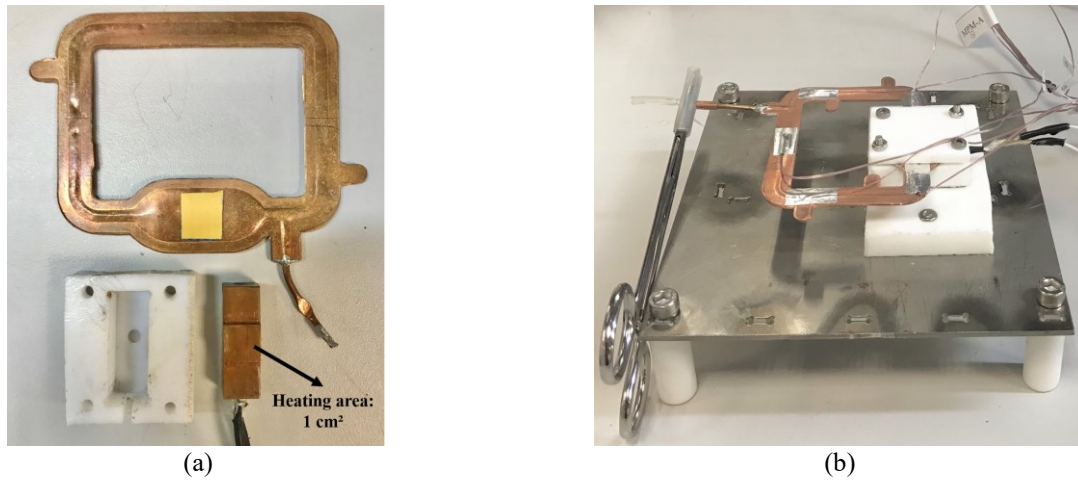


Figure 4. Workbench: (a) Details of the heater (b) UTLHP at operating conditions.

Tests are performed at horizontal orientation (non-assisted by gravity force), as shown in Figure 4(b). The room temperature is maintained at 24 ± 1 °C. The power input started at 0.5 W, reaching the maximum of 8 W, in several steps. The experiment was turned off when the evaporator temperature attained 100 °C, due to safety conditions for electronics (MAYDANIK *et al.*, 2011).

3.1 Data reduction

The thermal performance of the heat transfer devices can be evaluated by the overall thermal resistance, R_{UTHP} [°C/W], defined as:

$$R_{UTHP} = \frac{T_{ev} - T_c}{q} \quad (1)$$

where q is the power input rate [W], T_{ev} is the evaporator temperature (thermocouple T₁) [°C], and T_c is the condenser temperature (thermocouple T₄) [°C].

3.2 Uncertainty analysis

The experimental uncertainties are related to the temperature sensors, data logger and power supply errors (HOLMAN, 2011). As a result, the thermal resistance uncertainty is calculated as:

$$u(R_{UTLHP}) = \left(2 \left[\frac{1}{q} u(T) \right]^2 + \left[\frac{1}{q^2} u(q) \Delta T \right]^2 \right)^{1/2} \quad (2)$$

where $u(T)$ is the temperature uncertainty, $u(q)$ is the heat input uncertainty and ΔT is the temperature difference between the evaporator and condenser. The temperature uncertainty is estimated at ± 0.73 °C.

4. RESULTS AND DISCUSSION

Usually, the initial parameter used to evaluate the thermal performance of an UTLHP is the startup process. The evaporation phenomena of the working fluid occur when heat is applied to the outer surface of the evaporator. The vapor generated leaves the evaporator region through the vapor line to the condenser, increasing the inlet condenser temperature. Removing the heat at the condenser region, the vapor condensates and the resulting liquid moves back to the evaporator, pumped by the capillary pressure provided by the liquid line wick structure.

The temperature readings as a function of time for the several power steps, for the UTLHP in the horizontal orientation, filled with FR30% of water, is shown in Figure 5. The data does not indicate evaporator temperature overshoot. The startup happened at 3 W and the maximum heat input tested was 8 W before the evaporator temperature reached 100 °C (safety conditions for electronics). The temperatures of the evaporator outlet (T_2), condenser inlet (T_3) and condenser (T_4) are very close among themselves but further from the evaporator temperature (T_1). After 5 W, one can see that the two-phase change phenomena overcome the heat transfer conduction through the evaporator to the liquid line, i.e., the T_5 temperatures are higher than T_6 .

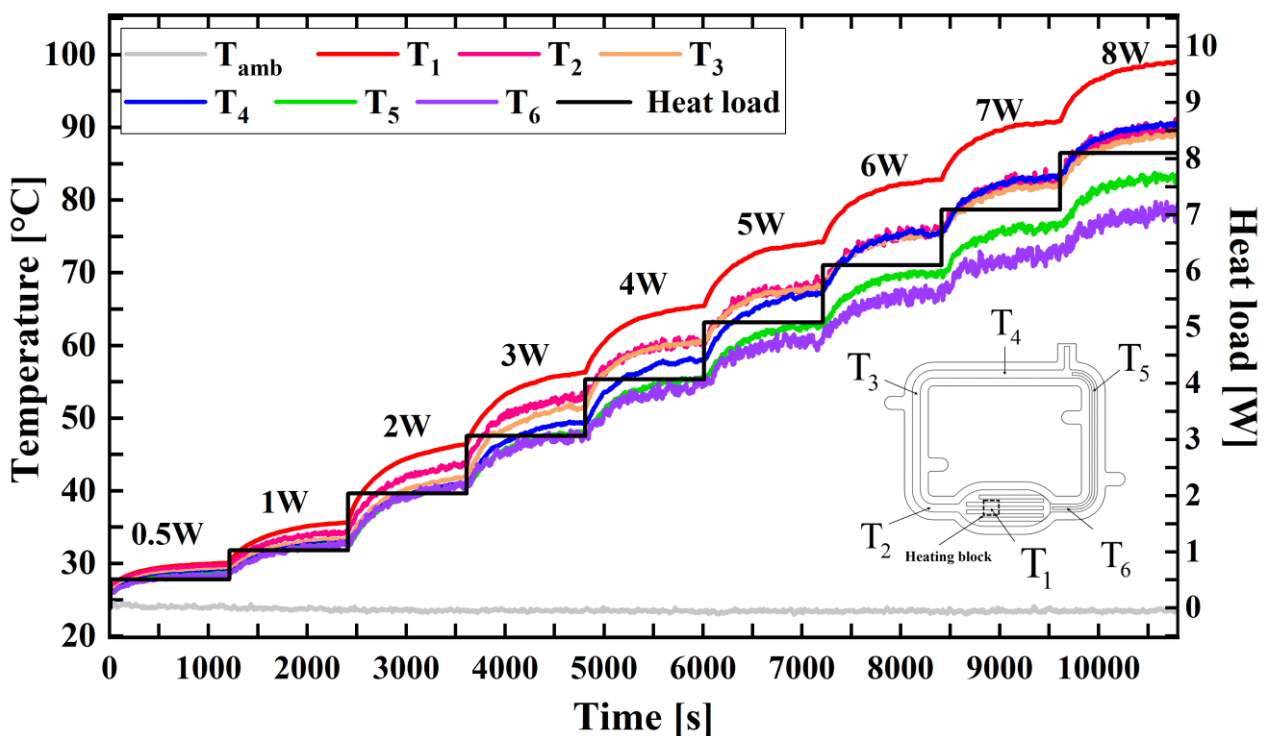


Figure 5. Temperature distribution of the UTLHP.

Figure 6 shows the average temperature of the UTLHP during steady-state operation (no apparent temperature oscillations occur) in the horizontal orientation. When the heat load applied increases, the temperature difference between the evaporator (T_1) and the condenser (T_4) decreases. On the other hand, the temperature difference between the evaporator outlet (T_2) and evaporator inlet (T_6) increases.

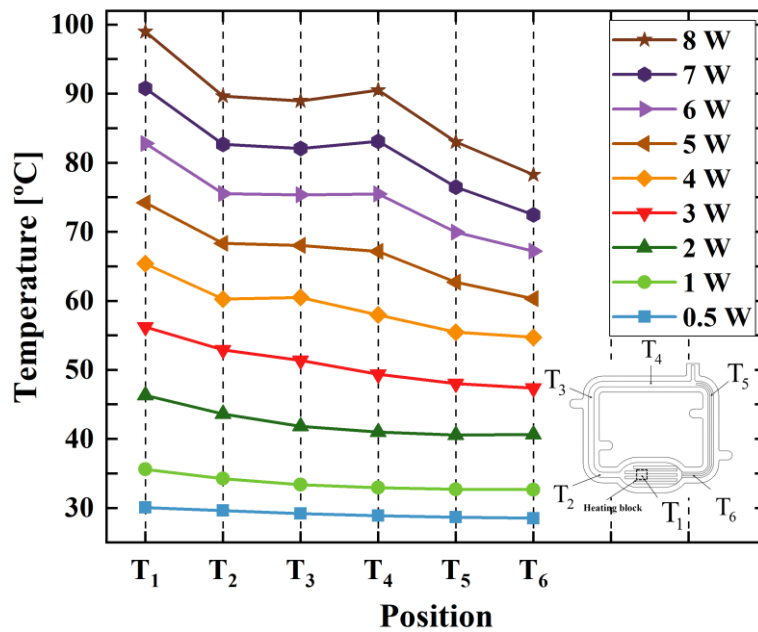


Figure 6. Average temperature of the UTLHP during steady-state operation for each heat load.

Figure 7 illustrates the temperatures of the UTLHP as a function of the heat load applied to the evaporator surface. For better visualization of the results, two plots are presented for two power input ranges. Above 3 W, the condenser temperature (T_4) overcomes the evaporator inlet temperature (T_6), as shown in Figure 7(a). This is not desired and shows that the heat is being conducted through the material (parasitic heat conduction). At 5 W (see Figure 7(b)), the condenser outlet temperature (T_5) exceeds the evaporator inlet temperature (T_6), showing that vapor reached the liquid line wick structure. Furthermore, increasing the applied heat input, the discrepancy between the temperatures T_4 and T_2 and the evaporator inlet temperature (T_6) becomes larger, showing that the parasitic heat conduction from the evaporator to the liquid line is overpassed by the two-phase change phenomenon.

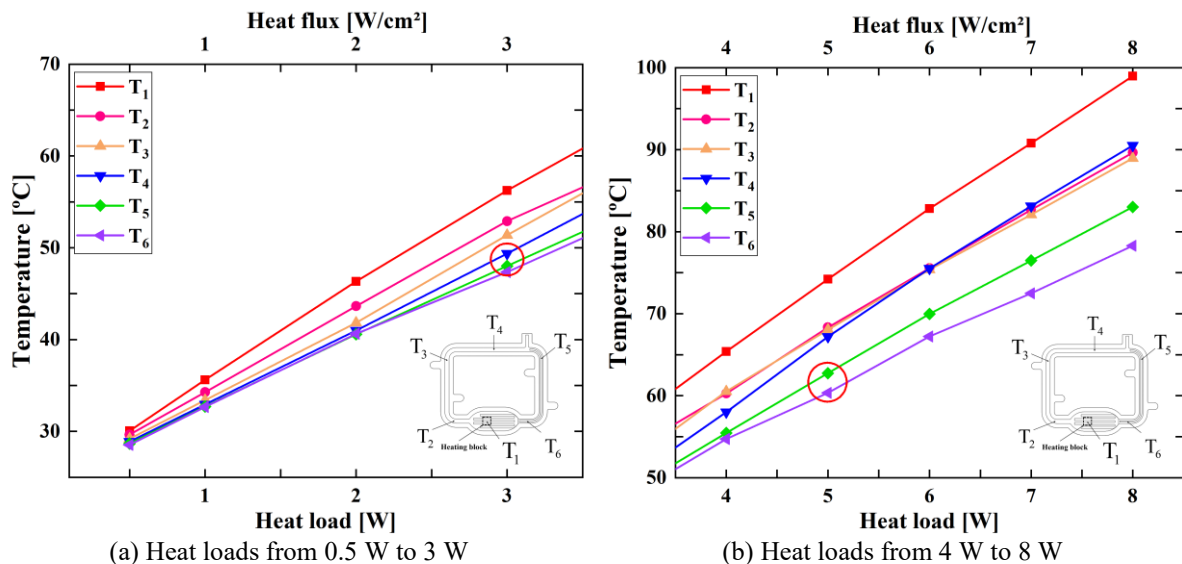


Figure 7. Temperature of the UTLHP as a function of the heat load applied to the evaporator.

Figure 8 illustrates the dependence of the thermal resistance on the heat power input. Above 2 W, the thermal resistance decreases sharply. The thermal resistance reached a minimum value of 1.05 °C/W at the 8 W of heat load. This behavior can be explained as follows: at low heat fluxes (below 3 W/cm²), the small amount of generated vapor results in a low mass flow rate, requiring only a minor fraction of the condenser length to dissipate the heat to the environment by natural air convection. At this time, the condenser is mostly occupied with the liquid phase, resulting in a high-temperature

difference between the evaporator and condenser. As the heat flux increases, increasing the mass flow rate, the condenser becomes filled with more vapor, decreasing the temperature difference between the evaporator and condenser.

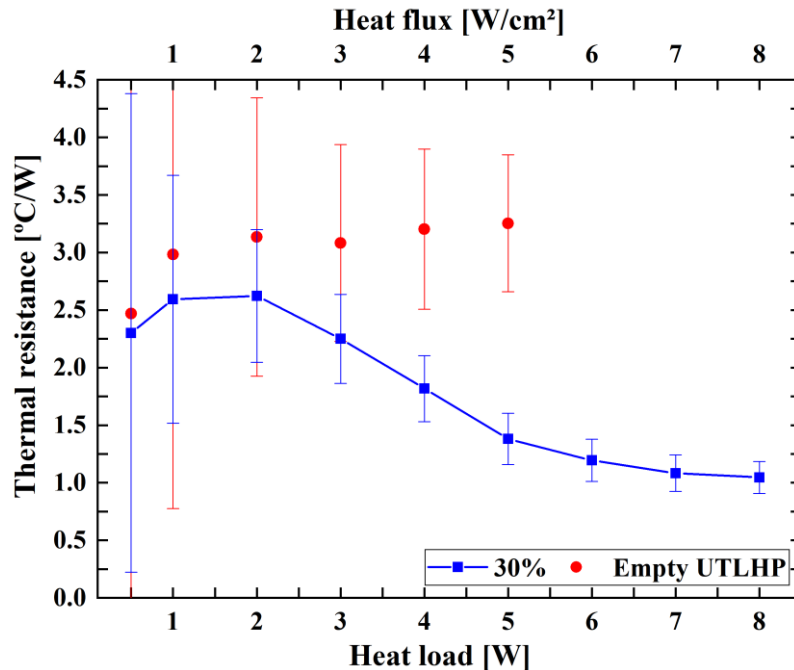


Figure 8. UTLHP thermal resistance in the horizontal orientation.

5. CONCLUSIONS

This work developed an ultra-thin loop heat pipe with 1.6 mm of thickness, fabricated by sintering processing and diffusion bonding. The test procedure could evaluate the heat transfer performance of the proposed UTLHP operating in the horizontal orientation under natural air convection with water as the working fluid. The experimental testing system was developed with an active area of 1 cm² to simulate a mobile electronic application. The conclusions are summarized as follows:

1. The sintering process and diffusion bonding caused low deformations in the ultra-thin loop heat pipe in 1.6 mm of thickness, keeping the designed geometry of the device.
2. Two wick structures located at the evaporator and the liquid line provided the driven force necessary to pump the working fluid through the device.
3. The proposed heat transfer device operated at a low heat flux of 3 W/cm² up to 8 W/cm² in the horizontal orientation, with an evaporator temperature of 56.2 °C and 99 °C, respectively.
4. The ultra-thin loop heat pipe achieved a thermal resistance of 1.05 °C/W at a heat input level of 8 W.
5. Although still demands development, the suggested ultra-thin loop heat pipe is a promising thermal management solution for mobile phones' application.

6. ACKNOWLEDGEMENTS

Acknowledgments are provided to the CNPq (Conselho Nacional de Desenvolvimento Científico e Tecnológico) and the UFSC (Universidade Federal de Santa Catarina) for their support.

7. REFERENCES

- Bejan, A., Kraus, A. D., 2003. *Heat Transfer Handbook*. Hoboken, New Jersey: John Wiley & Sons, Inc.
- Holman, J. P., 2011. *Experimental methods for engineers*, 8th ed. New York, USA.
- Maydanik, Y., Vershinin, S., Chernysheva M., Yushakova, S., 2011. "Investigation of a compact copper-water loop heat pipe with a flat evaporator". *Applied Thermal Engineering*, Vol. 31, No. 16, pp. 3533–3541.
- Maydanik, Y. F., 2005. "Loop heat pipes". *Applied Thermal Engineering*, Vol. 25, pp. 635–657.
- Mera, J. P. F., 2016. *Heat and Mass Transfer Analysis of a Copper Loop Heat Pipe*. Doctoral Dissertation, Graduate Program in Mechanical Engineering, Federal University of Santa Catarina, Florianópolis, Brazil.
- Nguyen, T., Mochizuki, M., Mashiko, K., Saito, Y., Sauciu, L., Boggs, R., 2000. "Advanced cooling system using

miniature heat pipes in mobile PC". *IEEE Transactions on Components and Packaging Technologies*, Vol. 23, No. 1, pp. 86–90.

TANG, H., Tang, Y., Wan, Z., Li, J., Yuan, W., Lu, L., Li, Y., Tang, K., 2018. "Review of applications and developments of ultra-thin micro heat pipes for electronic cooling". *Applied Energy*, Vol. 223, No. January, pp. 383–400.

Vasiliev Jr, L., Rabetsky, M., Kulakov, A., Vasiliev, L., Li, Z. M., 2008. "An advanced miniature copper heat pipes development for cooling system of mobile PC plataform". In *VII Minsk International Seminar "Heat Pipes, Heat Pumps, Refrigerators, Power Sources"*. Minsk, Belarus.

Vasiliev, L. L., 2008. "Micro and miniature heat pipes - Electronic component coolers". *Applied Thermal Engineering*, Vol. 28, No. 4, pp. 266–273.

Wikichip, 2021. *Semiconductor & Computer Engineering*. <https://en.wikichip.org/wiki/WikiChip>. Accessed 26 May 2021.

Zhou, W., Peida, X., Li, Y., Yan, Y., Li, B., 2017. "Thermal performance of ultra-thin flattened heat pipes". *Applied Thermal Engineering*, Vol. 117, pp. 773–781.

8. RESPONSIBILITY NOTICE

The authors are the only responsible for the printed material included in this paper.